

# A Systems Pharmacology Model for Drug Delivery to Solid Tumors by Antibody-Drug Conjugates: Implications for Bystander Effects

## Supplementary Information

Jackson K. Burton, Dean Bottino, and Timothy W. Secomb

### Governing equations

**Plasma pharmacokinetics.** The time course of plasma concentration  $C_{plasma}$  for a bolus dose of ADC in each vessel flowing into the network is represented by two-phase exponential kinetics

$$C_{plasma} = C_0 (\alpha 2^{-t/\tau_\alpha} + \beta 2^{-t/\tau_\beta}) \quad (1)$$

where  $t$  is time,  $C_0$  is the initial plasma concentration of ADC,  $\alpha$  and  $\beta$  are the fractions of the two clearance phases, and  $\tau_\alpha$  and  $\tau_\beta$  are the elimination half-lives in the two phases.

Concentration of ADC in the plasma is calculated using a molecular weight of 150 kDa and assuming mouse blood volumes between 1.5 and 2 mL.

**Transport by blood vessels.** ADC entering the tumor tissue from the circulation or free payload entering the circulation from tissue is transported by blood vessels. The concentration of solute  $p$  in each vessel, where  $p$  is ‘ADC’ or ‘payload’, is represented as a function  $C_p^v$  of time  $t$  and distance  $s$  along the vessel. The superscripts  $v$  and  $e$  denote ‘vessel’ and ‘extracellular’ respectively. Transport along the vessel is assumed to occur by convection, and the flux  $q_p^v$  of solute across vessel walls is assumed to be proportional to the concentration difference, with permeability  $P_p$ . By conservation of mass

$$A \frac{\partial C_p^v}{\partial t} + Q \frac{\partial C_p^v}{\partial s} = -q_p^v(s, t) = -2\pi r P_p (C_p^v - C_p^e) \quad (2)$$

where  $A$  is the vessel cross-sectional area,  $Q$  is the volume flow rate,  $r$  is the vessel radius, and  $C_p^e$  is the concentration of solute  $p$  in the tissue at the vessel-tissue interface. The sign of  $q_p^v$  indicates whether the solute is entering the tumor or being washed out by vessels.

**Transport in the tissue.** Transport of solutes within the extracellular tissue space is assumed to occur by passive diffusion, and effects of convective transport in tissue are neglected. The superscript  $t$  denotes ‘tissue’. For solute  $p$ , Fick’s second law and conservation of mass give

$$\frac{\partial C_p^t}{\partial t} - D_p \nabla^2 C_p^t = R_p(C_1^t, C_2^t, \dots, C_{N_s}^t) \quad (3)$$

where  $C_p^t(\mathbf{x}, t)$  is the tissue concentration at a point  $\mathbf{x}$  and time  $t$ ,  $D_p$  is the (uniform) tissue diffusivity, and  $R_p$  are the rates of reactions that, in general, depend on the concentrations of all  $N_s$  solutes, both diffusible and non-diffusible. The reactions included in this model are ADC binding to antigen, ADC-antigen internalization, catabolism of internalized ADC-antigen complex to free payload, payload efflux from the cell, and free payload uptake. The time course for non-diffusible solutes has the form of Eq. 3 except that diffusive term  $D_p \nabla^2 C_p^t$  is absent. The

specific equations formulated for ADC diffusion in the tumor tissue and reaction kinetics including bystander effects are specified in the methods section. Explicit models for intracellular trafficking, such as those described by (41), are not included, but could readily be incorporated in the model.

**Boundary conditions.** The three-dimensional tissue region that includes the vessel network is denoted by  $\Omega$ . In order for  $\Omega$  to be a representative region of the tumor, the net diffusive exchange of solute across the boundary of  $\Omega$  should be zero, otherwise the region would act as a net source or sink of solutes to or from the surrounding tissue. Application of the divergence theorem to Eq. 3 then yields the following condition

$$\int_{\Omega} \left( \frac{\partial C_p^t}{\partial t} - \Psi_p(\mathbf{x}, t) \right) dV = 0, \quad (4)$$

where  $\Psi_p$  represents the distribution of sources and sinks, including reactions in the tissue as defined by  $R_p$  in Eq. 3 and exchange with vessels.

**Solution method.** Equations 2-4 form the problem to be solved to simulate the transport and kinetics of ADCs in solid tumors. For diffusible solute  $p$ , a Green's function method is used to solve Eq. 3:

$$C_p^t(\mathbf{x}, t) = \int_0^t \int_{R^3} G_p(\mathbf{x} - \mathbf{x}^*, t - t^*) \Psi_p(\mathbf{x}^*, t^*) d\mathbf{x}^* dt^* + C_{0p}^t(\mathbf{x}) \quad (5)$$

where  $C_{0p}^t(\mathbf{x})$  is the initial concentration of solute  $p$  in the tissue. The Green's function  $G_p$  gives the contribution of concentration at position  $\mathbf{x}$  and time  $t$  resulting from production or release of solute at another position  $\mathbf{x}^*$  and at earlier time  $t^*$ . For non-diffusible solutes, solutions are obtained by integrating the local reactions  $R_p$  with respect to time. This solution is coupled with Eqs. 2 and 4, and the resulting system is discretized and solved numerically. Details of the solution method are given in (26). In summary, the vessels are divided into short cylindrical segments, each of which represents a discrete solute source or sink given by  $q_p(s, t)$  at distance  $s$  along the vessel centerline at time  $t$  (**Figure S1**). For time-dependent diffusion, the unsteady Green's function  $G_p(\mathbf{x} - \mathbf{x}^*, t - t^*)$  is defined as the concentration at point  $\mathbf{x}$  and time  $t$  resulting from an instantaneous unit source at a point  $\mathbf{x}^*$  at an earlier time  $t^*$ . It satisfies

$$\frac{\partial G_p}{\partial t} - D_p \nabla^2 G_p = \delta_3(\mathbf{x} - \mathbf{x}^*) \delta(t - t^*)$$

where  $\delta_3$  and  $\delta$  are Dirac delta functions in one and three dimensions. The solution that decays to zero at infinity for  $t > t^*$  is the Green's function:

$$G_p(\mathbf{x} - \mathbf{x}^*, t - t^*) = [4\pi D_p(t - t^*)]^{-3/2} \exp[-r^2/(4D_p(t - t^*))]$$

where  $r = |\mathbf{x} - \mathbf{x}^*|$ . The solution to the time-dependent diffusion equation in terms of the Green's function is shown in Eq. E. This equation is solved simultaneously with Eqs. B and D using the computational method (26), as summarized in the flow chart (**Figure S2**).

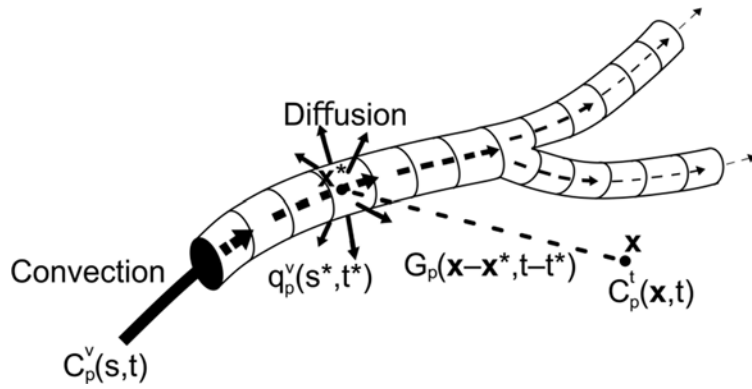


**Figure S1. Schematic diagram of Green's function method.** Solute is transported by convection along blood vessels, and diffuses through vessel walls and into surrounding tissue. The effect on the concentration of solute  $p$  at a point  $\mathbf{x}$  and time  $t$  in the tissue of a vessel source of solute at an earlier time  $t^*$  and position  $\mathbf{x}^*$  is given by the Green's function  $G_p(\mathbf{x} - \mathbf{x}^*, t - t^*)$ .

**Computational implementation.** The computational method has been described previously (26). The vessels are divided into short cylindrical segments, each of which represents a discrete solute source or sink. Convective transport of solute is simulated by explicitly tracking the displacement of fluid elements to determine the time-dependent solute concentration in each vessel segment. The concentration is dependent on the interaction between convective transport of the solute within vessels and diffusion in the surrounding tissue. The tissue concentration field for the diffusible solutes is constructed as a superposition of fields resulting from the vascular sources and from the reaction rates at a set of points distributed in the tissue, by utilizing the Green's function for the unsteady diffusion equation. The output of the model provides the time course of concentration for each solute at each tissue point in the network. For graphical output, contour plots of the concentration fields are created for a plane intersecting the microvessel network, with the entire network projected on the plane for visual reference.

**Figure S2.** Flow chart summarizing steps in the computational method using the unsteady Green's function approach.

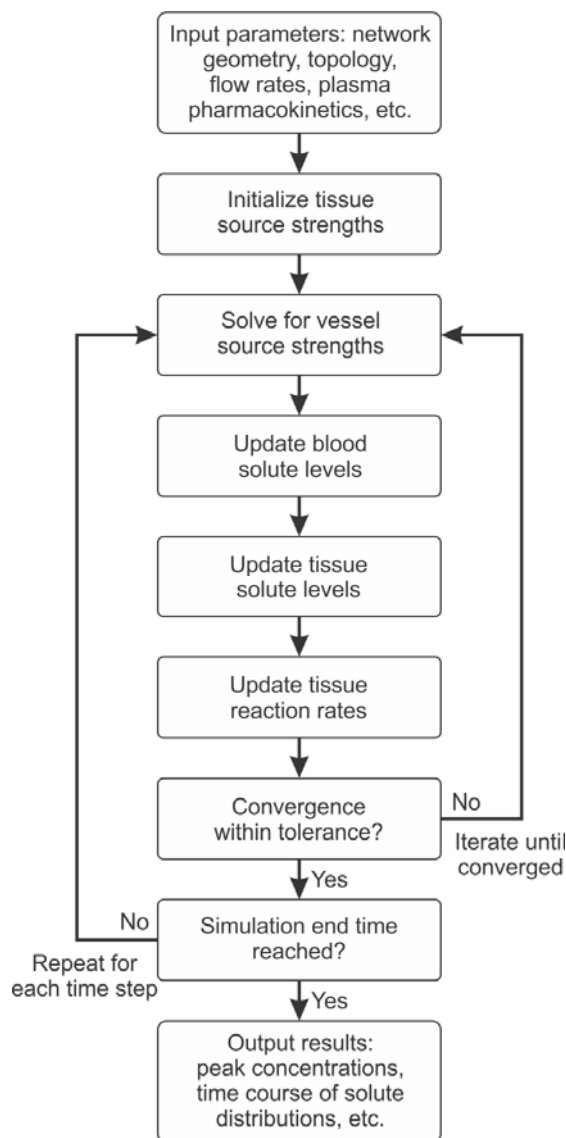


**Table S1: Parameters used for validation**

For each ADC property (antibody, linker, payload) and tumor specific property (cell line, antigen), the extent to which values in the literature matched the experimental setup in the test case were recorded. In several cases, different values for the same parameter were reported. Values for these parameters may have been substantially different and selection for use in the model was based on matching various properties to the test case to the extent the data was permitting. For example, the rate  $k_{on}$  used for the Rhoden et al. simulation was chosen from the literature because the measured value used the sm3e – CEA antibody-antigen complex. AG = antigen, AB = antibody, L = linker, PL = payload, CL = cell line. Check mark: parameter value from a study that matches the experimental condition in the model validation cases. Blank: mismatch. Dash: not applicable.

Parameter	Units	Description	Rhoden et al. (Figure 3)						Alley et al. (Figure 4A)						Li et al. (Fig. 4B cAC10, Fig. 4 C)						Li et al. (Fig. 4B: h116)									
Transport Parameters			Value	AG	AB	L	PL	CL	Ref.	Value	AG	AB	L	PL	CL	Ref.	Value	AG	AB	L	PL	CL	Ref.	Value	AG	AB	L	PL	CL	Ref.
$D_{ADC}$	$\mu\text{m}^2/\text{s}$	Diffusivity of ADC	25.4	✓	✓	-	-	✓	10	25.4							25.4						10	25.4						10
$D_{payload}$	$\mu\text{m}^2/\text{s}$	Diffusivity of free payload	-	-	-	-	-	-	-	-	-	-	-	-	-	-	$1 \times 10^{-6}$						A	$1 \times 10^{-6}$						A
$P_{ADC}$	$\mu\text{m}/\text{s}$	Vessel permeability to ADC	$3.87 \times 10^{-3}$	✓	✓	-	-	✓	10	$3.87 \times 10^{-3}$						10	$3.87 \times 10^{-3}$						10	$3.87 \times 10^{-3}$						10
$P_{payload}$	$\mu\text{m}/\text{s}$	Vessel permeability to payload	-	-	-	-	-	-	-	-	-	-	-	-	-	-	-							0.122						26
Kinetic Parameters																														
$k_{on}$	$(\text{nM s})^{-1}$	AB to AG association rate	$2 \times 10^{-4}$	✓	✓	-	-	✓	10	$2.8 \times 10^{-4}$	✓					15	$4.6 \times 10^{-4}$	✓	✓				18	$2.8 \times 10^{-4}$	✓		✓	✓	✓	15
$k_{off}$	$\text{s}^{-1}$	ADC dissociation rate from AG	$1.25 \times 10^{-6}$	✓	✓	-	-	✓	9	$4.7 \times 10^{-6}$	✓					15	$1.1 \times 10^{-3}$	✓	✓				18	$4.7 \times 10^{-6}$	✓		✓	✓	✓	15
$k_{int}$	$\text{s}^{-1}$	AB internalization rate	$1.38 \times 10^{-5}$	✓	✓	-	-	✓	9	$3.2 \times 10^{-4}$	✓					16	$7.09 \times 10^{-6}$	✓	✓				20	$3.2 \times 10^{-4}$	✓					16
$k_{deg}$	$\text{s}^{-1}$	AB degradation rate	-	-	-	-	-	-	-	$8.79 \times 10^{-6}$			✓			4	$9.8 \times 10^{-5}$		✓	✓			19	$9.8 \times 10^{-5}$		✓	✓	✓	✓	19
$k_{in}$	$\text{s}^{-1}$	cellular uptake of free payload	-	-	-	-	-	-	-	-	-	-	-	-	-	-	$2.31 \times 10^{-3}$		✓	✓			19	$2.31 \times 10^{-3}$		✓	✓	✓	✓	19
$k_{out}$	$\text{s}^{-1}$	cellular release of free payload	-	-	-	-	-	-	-	$4.16 \times 10^{-6}$			✓			4	$5.52 \times 10^{-5}$		✓	✓			19	$5.52 \times 10^{-5}$		✓	✓	✓	✓	19
Tumor Parameters																														
$C_{total}$	nM	Total antigen concentration	332	-	-	-	-	✓	10	440	-	-	-	-	✓	16	460,229	-	-	-	✓	21	23.2	-	-	-	-	✓	21	
$\varphi_e$	-	Extracellular volume fraction	0.4							0.4							0.4							0.4						
$\varphi^+$	-	Ag <sup>+</sup> cell volume fraction	0.6							0.6							0.6							0.6						
$\varphi^-$	-	Ag <sup>-</sup> cell volume fraction	0							0							0							0						
Plasma PK Parameters																														
$\alpha$	-	fraction of ADC phase clearance	0.204	✓	✓	-	-	✓	10	0.51	✓	✓	✓	✓	✓	17	0.52	✓	✓	✓	✓	✓	23	0.51		✓				17
$\beta$	-	fraction of phase clearance	0.796	✓	✓	-	-	✓	10	0.59	✓	✓	✓	✓	✓	17	0.48	✓	✓	✓	✓	✓	23	0.59		✓				17
$\tau_\alpha$	hr	Half-life of alpha phase	0.16	✓	✓	-	-	✓	10	1.84	✓	✓	✓	✓	✓	17	1.48	✓	✓	✓	✓	✓	23	1.84		✓				17
$\tau_\beta$	hr	Half-life of beta phase	28.88	✓	✓	-	-	✓	10	58.88	✓	✓	✓	✓	✓	17	151.8	✓	✓	✓	✓	✓	23	58.88		✓				17
ADC specific Parameters																														
$DAR_0$	-	Initial DAR value	-	-	-	-	-	-	-	2.3	-	-	-	-	-	17	4	-	-	-	-	21	4	-	-	-	-	-	21	
$a_{DAR}$	-	fraction of DAR phase clearance	-	-	-	-	-	-	-	0.174	✓	✓	✓	✓	✓	17	0.1	✓	✓	✓	✓	✓	23	0.1		✓	✓	✓	✓	23
$\beta_{DAR}$	-	fraction of DAR phase clearance	-	-	-	-	-	-	-	0.846	✓	✓	✓	✓	✓	17	0.9	✓	✓	✓	✓	✓	23	0.9		✓	✓	✓	✓	23
$\tau_{a,DAR}$	hr	Half-life of phase	-	-	-	-	-	-	-	5.03	✓	✓	✓	✓	✓	17	1.03	✓	✓	✓	✓	✓	23	1.03		✓	✓	✓	✓	23
$\tau_{\beta,DAR}$	hr	Half-life of phase	-	-	-	-	-	-	-	377.5	✓	✓	✓	✓	✓	17	156.78	✓	✓	✓	✓	✓	23	156.78		✓	✓	✓	✓	23

### Estimation of ADC plasma pharmacokinetics and DAR deconjugation time course

The ADC pharmacokinetic (PK) parameters  $\alpha$ ,  $\beta$ ,  $\tau_\alpha$  and  $\tau_\beta$  and the parameters to describe the rate of deconjugation of payload from antibody in plasma were fitted to Eq. 1 using the routine lsqcurvfit in MATLAB v2014a. Data points were digitized from figures in the published studies (Table S2-S3).

**Table S2: Plasma PK**

Figure S1A in Li et al.	
Time (days)	Concentration (ng/ml)
0.16	21714.9
1.00	17557.5
2.99	9414.4
6.02	6862.7
10.02	4501.9
Fig 2A (h1f6) in Alley et al.	
Time (days)	Concentration (nM)
0.05	208.7
0.19	160.8
0.36	111.3
1.98	55.9
4.00	32.0
7.02	8.8
10.05	4.2

**Table S3: DAR time course**

Figure 2 in Alley et al.	
Time (days)	DAR
0.07	2.07
0.17	1.87
0.33	1.90
1.01	1.70
2.01	1.61
4.01	1.42
7.01	1.33
10.02	1.12
Figure 4C in Sanderson et al.	
Time (days)	DAR
0.013	5.17
0.14	4.62
0.99	4.04
2.97	3.58
5.98	2.45
8.97	1.70